Internal Rotational Motion of the Chloromethyl Group of the Jet-Cooled Benzyl Chloride Molecule

Ryu Matsumoto, Tadashi Suzuki, and Teijiro Ichimura*

Department of Chemistry and Materials Science, Tokyo Institute of Technology, 2-12-1 Ohokayama, Meguro, Tokyo 152-8551, Japan

Received: December 24, 2004; In Final Form: February 28, 2005

The mass-resolved resonance enhanced two-photon ionization spectra of jet-cooled benzyl chloride were measured. Some low-frequency vibronic bands around the S_1-S_0 origin band were assigned to transitions of the internal rotational mode of the chloromethyl group. The internal rotational motion was analyzed by using the one-dimensional free rotor approximation. The conformation in the S_1 state was found to be that in which the C−Cl bond lies in orthogonal to the benzene plane. For the species with *m*/*e* 126, the transition energy of the internal rotational bands corresponded well to the potential energy values of $V_2 = 1900$ cm^{-1} and $V_4 = 30$ cm^{-1} in the S_1 state and the reduced rotational constant *B* values 0.50 and 0.47 cm^{-1} in the S_0 and S_1 states, respectively. The *B* values obtained for the chlorine isotopomer (*m*/*e* 128) were slightly different. The S_1 potential barrier height was found to be about 3 times larger than that for the S_0 state. Molecular orbital calculations suggest that the difference between energies of the HOMO and LUMO with respect to the rotation of the chloromethyl group correspond approximately to the potential energy curve obtained for the S_1 state.

1. Introduction

The large-amplitude vibration has been of interest to many researchers due to its large anharmonicity. Large-amplitude vibrations, unlike any other normal mode vibrations, have quite low frequencies and it is presumed that they may affect the relaxation processes in the electronic excited state. However, the excitation spectrum of large molecules including the large-amplitude vibrational motion is very congested, so that interpretation can be difficult. The supersonic jet technique is thus very useful in obtaining information on the large-amplitude vibrations. Okuyama et al. observed the laser-induced fluorescence excitation spectra with this technique for the first time in the middle 1980s,[1] and since then, a number of groups have studied toluene derivatives.[2−8] The potential energy curve on the methyl internal rotational motion was estimated in the ground and excited states, and the drastic change of the potential barrier height upon the electronic excitation was shown. For chlorotoluenes[7] and methylanisoles[8] it is indicated that the internal rotational motion of the methyl group would promote intersystem crossing from the lowest excited singlet state. It can be concluded that the low-frequency motion of the methyl internal rotation should enhance the level mixing in the lowest triplet excited state.

The molecular structure and the barrier height for the internal rotation of benzyl derivatives in the ground state have also been studied by some groups. The ground-state structure has been investigated by using the NMR J method, electron diffraction, microwave spectroscopy, and IR/Raman spectroscopy.[9−16] Sorenson and True[15] measured low-resolution microwave spectra of benzyl halides and suggested that the conformation in the ground electronic state for all the benzyl halides they studied is not planar (the C−X bond lies out of the phenyl plane). Internal rotational motion of the ring-substituted benzyl alcohols was studied by Im et al.[17] with mass-resolved resonance-enhanced two-photon ionization spectroscopy. They showed that the barrier height in the S_1 state was 2 times more than that in the S_0 state.

Benzyl chloride is known for its unique reaction and relaxation dynamics in the electronic excited state: photoexcited benzyl chloride undergoes fast dissociation to give benzyl radical and chlorine atom.[18] Benzyl chloride has orthogonal conformation (the C−Cl bond lies in the plane perpendicular to the benzene plane) in the ground electronic state, and the potential barrier height of the internal rotational motion was 740 cm^{-1} in an electron diffraction experiment.[11,12] The internal rotational motion in benzyl chloride can be anticipated to contain information on the interaction between the phenyl group and the chloromethyl group; thus we considered it important to study the internal rotation of the chloromethyl group on benzyl chloride.

In this experiment, the mass-resolved resonance enhanced two-photon ionization (RE2PI) spectrum of the jet-cooled benzyl chloride was measured. Because the benzyl chloride consists of two isotopomers with respect to the chlorine atom, the isotopic effect should appear as a change in the rotational momentum of the internal rotation. Therefore, the mass-resolved RE2PI spectroscopy should give useful information on the internal rotation of the chloromethyl group. Analyses of the potential energy curves of the internal rotation in the S_1 state were performed by using a one-dimensional free rotor model. We discuss the barrier height with the results of molecular orbital (MO) calculations.

2. Experimental Section

A liquid sample of benzyl chloride (purity 99.5%) was purchased from Tokyo Kasei Co., Ltd. and used without further purification.

A schematic diagram of the experimental apparatus for the measurement of the RE2PI excitation spectrum in a supersonic free jet is shown in Figure 1. A pulsed tunable dye laser

* Corresponding author. E-mail: tichimur@cms.titech.ac.jp.

10.1021/jp044131o CCC: $30.25
Published on Web 03/30/2005

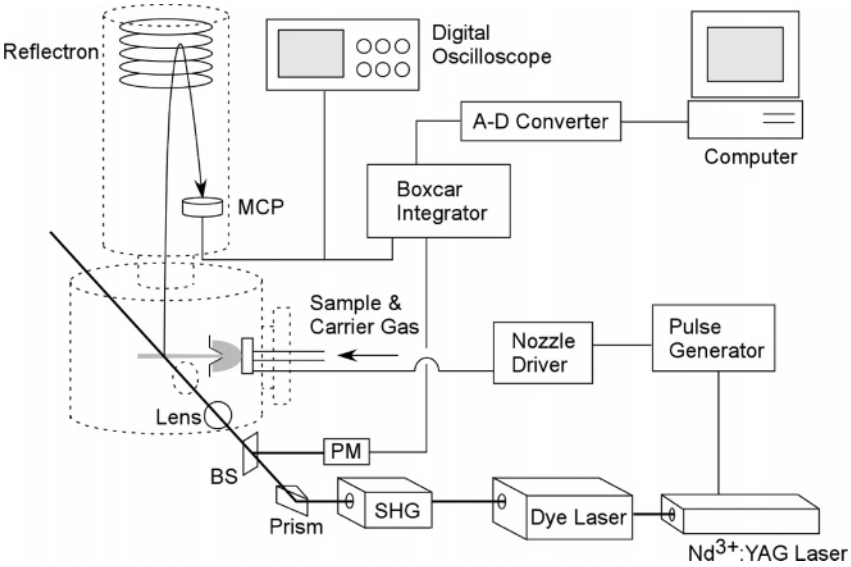

Figure 1. Schematic diagram of the experimental setup for the mass-resolved RE2PI spectroscopy: MCP, microchannel plate; SHG, second harmonic generator; PM, power meter; BS, beam splitter.

(Lambda Physik Scanmate IIE: Coumarin 153 in methanol/1,4-dioxane) pumped with the second harmonic of a Nd^{3+}:YAG laser (Continuum Powerlite 8010) was frequency doubled by a second harmonic generator (Inrad Autotracker-III). The energy resolution of the excitation laser was estimated to be about 0.02 cm^{-1}. The excitation laser was focused with a 1000 mm lens and was crossed with a skimmed molecular beam perpendicular to the direction of the beam. The excitation laser and the pulsed valve were synchronized with use of a digital delay pulse generator (Stanford Research Systems DG535).

The sample reservoir was heated to 300−330 K to obtain the required vapor pressure. The sample vapor was then seeded by 2 atm of Ar or N_2 gas. The gas mixture was expanded into the vacuum chamber, passing through a pulsed valve (General Valve Series 9, 0.8 mm diameter orifice) operated at 10 Hz. The supersonic free jet was skimmed with a 1.0 mm diameter skimmer positioned 12 mm downstream of the orifice. The background pressure of the ionization chamber was below 10^{-7} Torr without and about 10^{-5}−10^{-6} Torr with the pulsed valve operating, respectively. The background pressure of the flight tube was less than 10^{-6} Torr when the pulsed valve was in operation. The cations were mass-selected by the Wiley−McLaren style time-of-flight mass spectrometer and refrectron. For the detection of the ion, a microchannel plate (R. M. Jordan Co. 40 mm Z-Gap MCP) was used. To measure the RE2PI excitation spectrum, the signal from the detector was averaged by a boxcar integrator (Stanford Research Systems SR250), digitized by an A/D converter (Union Data UAD-98KJ or ADTEK AB98-05B), and then transferred to a personal computer (NEC PC-9801). The excitation laser power was simultaneously monitored with a handmade power meter and stored in the same way as the ion signal. On the measurement of the time-of-flight mass spectrum, the ion signal was averaged by a digital oscilloscope (LeCroy 9314C).

3. Analytical Treatment and Selection Rules

We analyze the treatment of the internal rotational motion of benzyl chloride as follows. The rigid chloromethyl group (C_s symmetry) is connected to the rigid phenyl group (C_{2v} symmetry) and the internal rotational motion is analyzed with the one-dimensional free rotor basis model.[19,20] The wave function, $\Psi(\phi)$, for the internal rotation should satisfy the following equations.

$$\left(-B\frac{\partial^2}{\partial\phi^2} + V(\phi)\right)\Psi(\phi) = E\Psi(\phi) \tag{1}$$

$$V(\phi) = \sum_n \frac{V_n}{2}(1 - \cos n\phi) \tag{2}$$

where B is the reduced rotational constant, V_n is the n-fold barrier height, and ϕ is the rotational angle between the benzene frame and the chloromethyl group, respectively. Here, the ϕ value is defined as the dihedral angle θ (C_{ortho}−C_{ipso}−C_{α}−Cl). In the case of the benzyl chloride, it is sufficient to use the terms of $n = 2m$ (m is a positive integer) because of its molecular symmetry. Since the higher terms are not so effective in describing the potential energy curve, the $n = 2$ and 4 terms were used here. The wave functions were expanded by the 51 free rotor wave functions Ψ_p as a basis set.

$$\Psi_p = \frac{1}{\sqrt{2\pi}}\exp(ip\phi) \qquad p = 0, \pm1, \pm2, ... \tag{3}$$

Substituting (1) with (3) and diagonalizing the resulting matrix gives the eigenfunctions and eigenvalues of the internal rotational motion.

Based on the molecular symmetry, the symmetry of the wave functions can be divided into four species, (s,s), (s,a), (a,s), and (a,a), where the former character in parentheses indicates that the wave function is symmetric or antisymmetric to the reflection to the plane perpendicular to the phenyl ring, and the latter character indicates the symmetry of the wave function to the plane of the ring. Since the product of the vibrational wave functions must be totally symmetric, the vibronic transition involving the internal rotation can occur when the vibrational levels belong to same symmetry species.

$$\text{(s,s)} \leftrightarrow \text{(s,s)},\ \text{(s,a)} \leftrightarrow \text{(s,a)},\ \text{(a,s)} \leftrightarrow \text{(a,s)}\ \text{and}\ \text{(a,a)} \leftrightarrow \text{(a,a)} \tag{4}$$

4. Results and Discussion

4.1. Mass-Resolved RE2PI Spectra. Figure 2 shows the mass-resolved RE2PI excitation spectrum of benzyl chloride

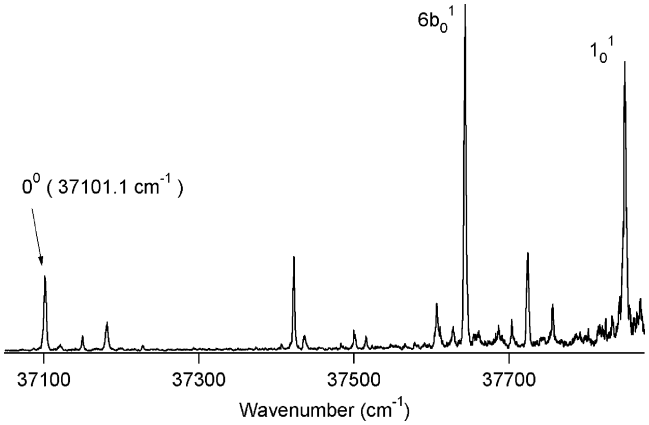

Figure 2. Mass-resolved RE2PI spectrum of the jet-cooled benzyl chloride monitored Bz^{35}Cl (*m*/*e* 126).

with *m*/*e* 126 (Bz^{35}Cl, hereafter). The observed spectrum was almost identical with the laser induced fluorescence excitation spectrum measured by Takemura et al.[21] The prominent band at 37101.1 cm^{-1} was previously assigned to the $S_1 \leftarrow S_0$ origin band and the bands at 0^0 +542.3 and +748.5 cm^{-1} were assigned to $6b_0^1$ and 1_0^1 vibronic bands, respectively. Some low-frequency bands were observed above the origin and also adjacent to each vibronic band. Figure 3 shows the expanded spectrum under the energy region around the origin band in different jet conditions. The band intensity of some transitions was found to differ according to the stagnation pressure of the carrier gas. We assign the observed vibronic bands A to H and summarize the excess energy of the bands in Table 1. It was found that the relative intensity of bands D, F, and H to the origin was constant under any jet conditions, while that of the other bands varied. Therefore, the former can be assigned to the vibronic bands of the bare benzyl chloride and the latter are presumed to result from the clusters or the hot bands. Since the sum of the excess energy of bands D and F approximately corresponds to that of band H, we can assign band H to a combination band of D and F.

We measured the time-of-flight mass spectrum with the wavelength of the excitation laser fixed at each band. All of the TOF mass spectra except for band A showed the intense peaks attributed to the benzyl chloride cations (*m*/*e* 126 and 128), while for band A excitation the relatively intense peaks of the benzyl chloride and Ar (*m*/*e* 166 and 168) cluster were observed. Band A disappeared when N_2 gas was used as a carrier. This band can thus be assigned to the 0^0 transition of the BzCl·Ar cluster. The benzyl chloride dimer cannot be observed in the mass spectra. Therefore the bands B, C, E, and G can be assigned to the hot band. From the energy relative to the origin band, the bands E and G can be assigned to the combinations of D with B and F with B, respectively. The two low-frequency transitions B and C are tentatively assigned to the hot bands of internal rotation of the chloromethyl group because it would be the most appropriate candidate for the lowest frequency vibration. We measured the mass-resolved RE2PI spectrum for the Bz^{37}Cl in order to investigate the isotope effect on the low-frequency vibrations. The results are also summarized in Table 1. It was found that the spacing of each band from the origin band was slightly reduced. The largest isotope shift was observed in band H.

Since the signal intensity of the 0^0 transition is larger than any other low-frequency vibrations, the conformation of the chloromethyl group in the S_1 state should be identical with that of the S_0 state, in orthogonal conformation.[11,12] To confirm the

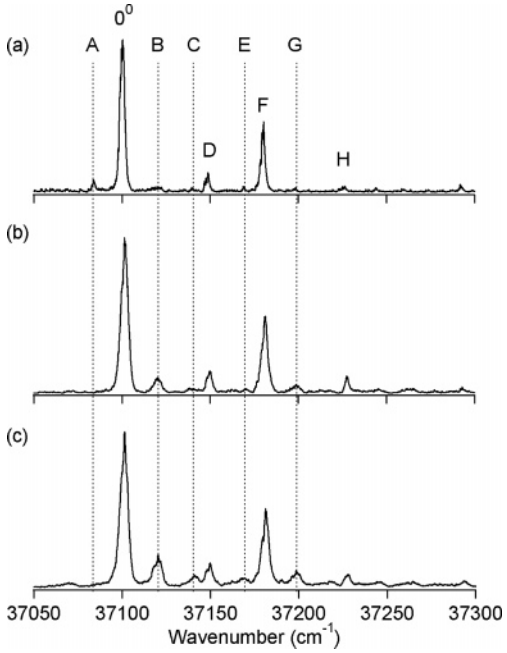

Figure 3. Mass-resolved RE2PI spectra (*m*/*e* 126) with stagnation pressures of (a) 4.0, (b) 1.8, and (c) 0.6 atm.

TABLE 1: Energy and Assignment of Low-Frequency Bands Observed around the S_1-S_0 Origin Band

band	assignment	Bz^{35}Cl (cm^{-1})	Bz^{37}Cl (cm^{-1})
A	BzCl·Ar 0^0	−14.8	*a*
0^0		37101.1	37102.0
B	T_1^1	+19.2	+18.9
C	T_2^2	+39.9	+39.6
D	$10b_0^1$	+48.3	+47.7
E	$10b_0^1T_1^1$	+67.7	+66.5
F	$16b_0^1$	+80.0	+79.3
G	$16b_0^1T_1^1$	+97.5	+97.1
H	$10b_0^116b^1$	+126.2	+124.5

[a] The band A for Bz^{37}Cl could not be observed because the band intensity was very weak.

minimum energy conformation, molecular orbital calculations were carried out. The geometry of the S_0 and S_1 state was optimized at B3LYP/6-31G(d,p) and CIS/6-31G(d,p), respectively, using the Gaussian 98 package.[22] The calculated geometry of the S_0 state is almost similar to the results of Benassi et al. calculated with the MP2 method.[16] The optimized geometries in both states were found to be in the orthogonal conformation and in C_s molecular symmetry. No other local minimum was found for the chloromethyl internal rotation. These calculations thus support our speculation on the conformation. The energy levels of the internal rotation should be doubly degenerated with respect to the reflection of the benzene plane. The even number levels have (s,s) and (s,a) symmetry and the odd number levels have (a,s) and (a,a) symmetry. The selection rules should be even ↔ even and odd ↔ odd.

Therefore we assigned the hot bands B and C to T_1^1 and T_2^2, respectively (T denotes the internal rotational mode). On the basis of this assignment we simulated the transition energies of the internal rotational mode as described in section 3. We assumed the potential terms of the S_0 state were identical to those obtained by electron diffraction measurement,[11,12] $V_2 = 740$ and $V_4 = 0$ cm^{-1}. The other parameters, the B values in both states and the V_2 and V_4 values in the S_1 state, were fitted to the observed transition energies. For Bz^{35}Cl the best fitting was obtained with the B values 0.50 and 0.47 cm^{-1} in the S_0

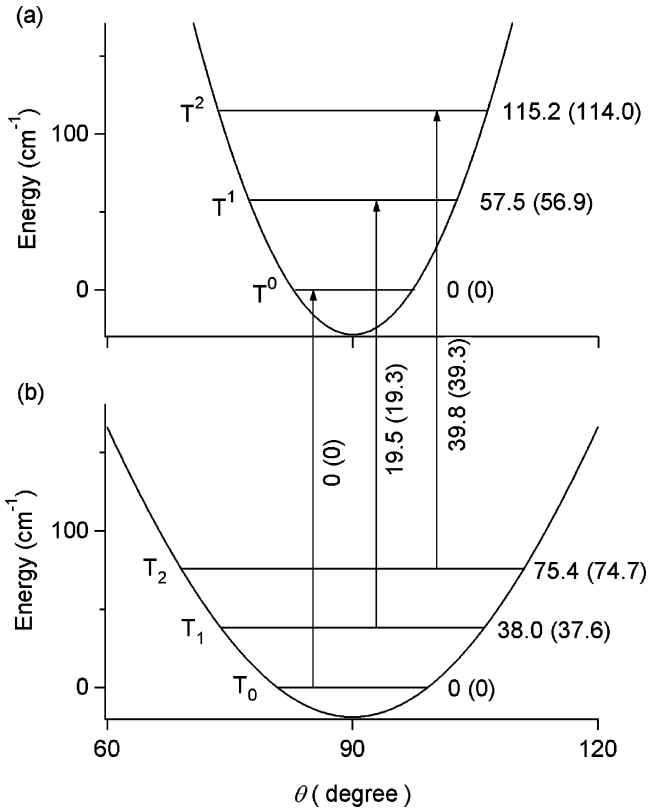

Figure 4. Relative energies for the vibrational levels of the internal rotation in (a) S_1 and (b) S_0 states. The observed transitions are indicated by the arrows. The values for the $Bz^{37}Cl$ are described in parentheses.

TABLE 2: The Observed and Calculated Transition Energies Involving the Internal Rotational Mode

	$Bz^{35}Cl$ (cm^{-1})		$Bz^{37}Cl$ (cm^{-1})	
transitions	obsd	calcd[a]	obsd	calcd[b]
T_0^0	0	0	0	0
T_1^1	19.2	19.5	18.9	19.3
T_2^2	39.9	39.8	39.6	39.3

[a] $B(S_0) = 0.50$ cm^{-1}, $B(S_1) = 0.47$ cm^{-1}, $V_2 = 1900$ cm^{-1}, $V_4 = 30$ cm^{-1}. [b] $B(S_0) = 0.49$ cm^{-1}, $B(S_1) = 0.46$ cm^{-1}, $V_2 = 1900$ cm^{-1}, $V_4 = 30$ cm^{-1}.

TABLE 3: Calculated Franck−Condon Factors of the S_1-S_0 Transition[a]

	S_1 state			
S_0 state	T^0	T^1	T^2	T^3
T_0	100	0	4.5	0
T_1	0	79.9	0	5.8
T_2	0.6	0	80.5	0
T_3	0	5.7	0	62.8

[a] All values were normalized to the 0° transion as 100.

and S_1 states, respectively, and the potential energy terms $V_2 = 1900$ cm^{-1} and $V_4 = 30$ cm^{-1} in the S_1 state. The results of $Bz^{37}Cl$ were well reproduced by only changing the B values of both states and they were found to be 0.49 and 0.46 cm^{-1} in the S_0 and S_1 state, respectively. The decrease of the B values upon the electronic excitation would be due to the stretched length of the C−Cl bond. The tunneling splitting in every internal rotational level was obtained to be too small to be observed (<0.01 cm^{-1}). The observed and calculated transition energy was shown in Figure 4 and summarized in Table 2. The calculated Franck−Condon factor was listed in Table 3. The calculated values well satisfied the selection rules of the even ↔ even and odd ↔ odd transitions. The Franck−Condon factors of the T_1^1 and T_2^2 transitions are comparable to that of the T_0^0 transition, but the band intensity is too weak. This is due to the small populations in the higher levels. The vibrational temperature was estimated from the obtained energy level spacings and calculated Franck−Condon factors, and obtained to be about 40 K in the hottest spectrum (Figure 3c).

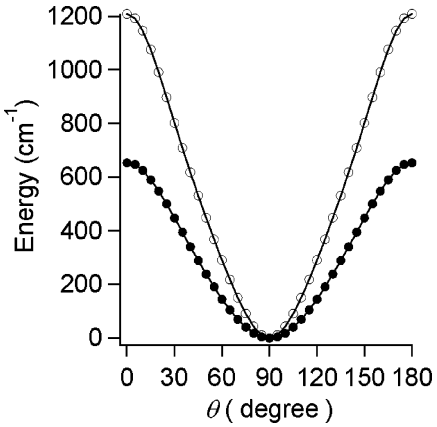

Figure 5. Potential energy curves in S_0 (filled circles) and S_1 (open circles) states obtained by MO calculations. Both are normalized to the energy minimum.

We conclude that the potential barrier height in the excited state is increased about 3 times larger than that in the ground state. The barrier height for the chloromethyl group is extraordinarily higher than that of the other benzyl derivatives.[17] The detailed discussion will be described in the following section.

4.2. Electronic Structure of the Benzyl Chloride. To investigate further the extremely high potential barrier height in the S_1 state, we performed MO calculations on the potential energy curve of the internal rotation of the chloromethyl group. The total energies in the ground and excited states were calculated by using the dihedral angles θ from 0° to 90° in a 5° step, as shown in Figure 5. The potential barrier heights were calculated as 654 cm^{-1} in the ground state and 1257 cm^{-1} in the excited state. Though the values calculated were lower than the observed ones, the calculation reproduced the experimental result whereby the barrier height increased upon electronic excitation.

Using the optimized geometry of the S_0 and S_1 states, we also carried out vibrational frequency calculations. The lowest frequency mode corresponds to the internal rotation mode of the chloromethyl group, whose frequency was calculated to be 38.2 cm^{-1} in the S_0 state and 53.7 cm^{-1} in the S_1 state. The second lowest frequency mode was the 10b mode vibration (bending mode between the phenyl and the chloromethyl groups), whose frequency was found to be 109.9 cm^{-1} in the S_0 state and 87.5 cm^{-1} in the S_1 state. The third one was the 16b mode and its frequency was calculated as 271.5 cm^{-1} in the S_0 state and 206.2 cm^{-1} in the S_1 state. The internal rotation was found to be the lowest frequency mode. The band C at 0^0 +48.2 cm^{-1} can be assigned to the $10b_0^1$ vibronic band, and the band D at 0^0 +80.0 cm^{-1} to the $16b_0^1$ vibronic band. When we compared the internal rotation bands to bands C and D, the smaller isotope shift was observed. This implies the fairly equal energy shifts in both the S_0 and S_1 states for the internal rotation modes. From this analysis, we conclude that the observed internal rotational bands are the hot bands.

The very high potential barrier height suggests that a strong interaction is occurring between the phenyl group and the chloromethyl in the excited state. Figure 6 shows the variation

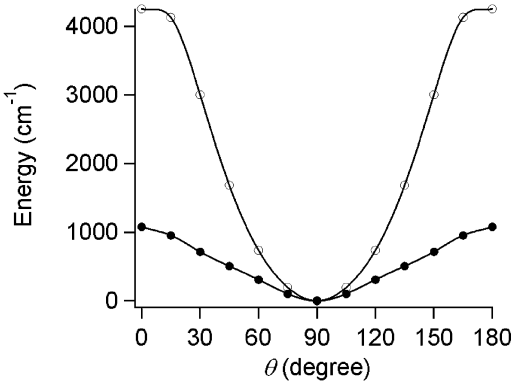

Figure 6. Energy variations of HOMO (filled circles) and LUMO (open circles) with the internal rotation. Both are normalized to the energy minimum.

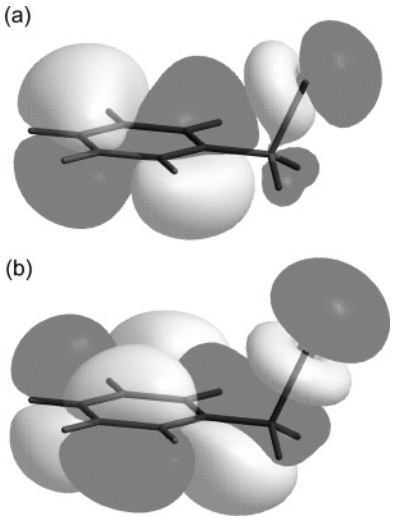

Figure 7. Calculated (a) HOMO and (b) LUMO of benzyl chloride in the ground-state geometry.

of the calculated energies of the HOMO and LUMO for different angles of the internal rotation. Both orbitals have their global minimum in the orthogonal conformation ($\theta = 90°$), and the differences in energies between the orthogonal and planar geometries ($\theta = 0°$) were found to be 1077 cm^{-1} in HOMO and 4254 cm^{-1} in LUMO. The energy difference between these orbitals corresponds approximately to the potential barrier height in the S_1 state. Therefore, we conclude the electronic structure of the LUMO is related to the internal rotational motion. The calculated HOMO and LUMO of benzyl chloride in the ground state geometry are shown in Figure 7. One can clearly see a strong interaction between the π^* orbital of the benzene ring and the σ^* orbital of the C−Cl bond in the LUMO. The resulting orbital spreads over the $C_{ipso}-C_\alpha$ bond and forms the bonding orbital between the phenyl group and the chloromethyl group. This interaction may be responsible for the extraordinarily high potential barrier in the excited state.

Theoretical study on the benzyl derivatives by Benassi and Taddei[23] suggested that the rotational barrier in the S_0 state is mainly controlled by the hyperconjugative effect of π(benzene)−$\sigma^*(C_\alpha-X)$ and π^*(benzene)−$\sigma(C_\alpha-X)$, where X = F and Cl. Our calculation proposes that π^*(benzene)−$\sigma^*(C_\alpha-X)$ interaction is effective to the rotational barrier in the excited state. In the planar conformation, there can be no interaction between the π^*(benzene) and the $\sigma^*(C_\alpha-Cl)$ because of symmetry restrictions. Therefore the energy difference in the planar conformation between the π^*(benzene) and the $\sigma^*(C_\alpha-Cl)$ was calculated to be about 7300 cm^{-1}, and should represent the zero-order energy difference between these levels in the orthogonal conformation. The strong interaction is thought to be caused by the energy proximity of these orbitals.

TABLE 4: The Barrier Height of the Internal Rotational Mode and the Dissociation Energy of the C−X Bond in the Benzyl Derivatives

	barrier height (cm^{-1})		dissociation energy (kJ/mol)[g]
	S_0 state	S_1 state	
toluene (Bz-H)	4.9[a]	25[b]	368
benzyl fuoride (Bz-F)	58.2[c]	<300[d]	
benzyl alcohol (Bz-OH)	140[d]	330[d]	322
benzyl chloride (Bz-Cl)	740[e]	1900[f]	289

[a] Reference 23. [b] Reference 24. [c] Reference 9. [d] Reference 17. [e] Reference 11. [f] This work. [g] Reference 25.

Table 4 shows the internal rotational barrier heights in the S_1 states of the toluene and some benzyl derivatives. The barrier heights for these molecules differ by the substituted groups. From the above discussion, we consider this is due to the difference in the interaction between the $\sigma^*(C_\alpha-X)$ orbital and π^*(benzene), and this would be roughly estimated by the energy difference of these levels. Since the energy level of the π^*-(benzene) can be assumed to be constant for each molecule, the interaction would depend on the energy level of the σ^*-$(C_\alpha-X)$, which almost corresponds to the dissociation energy of the $C_\alpha-X$ bond. Table 4 also shows the dissociation energy of the $C_\alpha-X$ bond. Since the energy level of the $\sigma^*(C_\alpha-H)$ in toluene is largely separated from that of the π^*(benzene) the barrier of the internal rotation is too small. For the benzyl derivatives smaller energy separations than toluene give rise to the interaction of π^*(benzene)−$\sigma^*(C_\alpha-X)$. The interaction in benzyl chloride should be strong because the energy difference is the smallest of four. Therefore the resulting bonding orbital causes the high barrier height of the internal rotation in the S_1 state.

5. Summary

The internal rotation of chloromethyl group on benzyl chloride in the S_1 state was investigated by mass-resolved resonance-enhanced two-photon ionization (RE2PI) excitation spectroscopy in a supersonic jet condition. We observed the low-frequency bands up to 150 cm^{-1} above the origin in the S_1 state. The low-frequency bands whose intensities varied with the supersonic jet condition were assigned to the internal rotational band of the chloromethyl group. The conformation in the S_1 state was clarified as that in which the C−Cl bond of benzyl chloride lies in the plane perpendicular to the benzene plane. Using the one-dimensional free rotor approximation the spectra were analyzed, and the potential energy terms were found to be $V_2 = 1900$ cm^{-1} and $V_4 = 30$ cm^{-1} in the S_1 state.

The rotational constant of the internal rotation for the Bz^{35}-Cl was found to be 0.50 cm^{-1} in the S_0 state and 0.47 cm^{-1} in the S_1 state. For $Bz^{37}Cl$, the B values were 0.49 and 0.46 cm^{-1} in the S_0 and the S_1 states, respectively. The potential barrier height was found to be about 3 times as high in the S_1 state as in the S_0 state. We also calculated the HOMO and LUMO of benzyl chloride. Both have their energy minimum in the orthogonal conformation and their maximum in the planar conformation where the C−Cl bond lies in the benzene plane. The MO calculations suggest the large energy difference (~4300 cm^{-1}) between the orthogonal and planar conformations in the LUMO. They also suggest that the LUMO of the orthogonal conformation consists of the π^* orbital of the benzene ring and

the σ^* orbital of the C−Cl bond, forming the strong bond between these orbitals. It is concluded that the stabilization of the LUMO in the orthogonal conformation should be caused by the interaction between the π^*(benzene) and the σ^*(C−Cl), which arises from the small energy separation of these levels.

References and Notes

(1) Okuyama, K.; Mikami, N.; Ito, M. *J. Phys. Chem.* **1985**, *100*, 5617.
(2) Breen, P. J.; Warren, J. A.; Bernstein, E. R.; Seeman, J. I. *J. Chem. Phys.* **1987**, *87*, 1917.
(3) Okuyama, K.; Mikami, N.; Ito, M. *Laser Chem.* **1987**, *7*, 197.
(4) Aota, T.; Ebata, T.; Ito, M. *J. Phys. Chem.* **1989**, *93*, 3519.
(5) Mizuno, H.; Okuyama, K.; Ebata, T.; Ito, M. *J. Phys. Chem.* **1987**, *91*, 5589.
(6) Fujii, M.; Yamauchi, M.; Takazawa, K.; Ito, M. *Spectrochim. Acta A* **1994**, *50*, 1421.
(7) Kojima, H.; Sakeda, K.; Suzuki, T.; Ichimura, T. *J. Phys. Chem.* **1998**, *102*, 8727
(8) Ichimura, T.; Suzuki, T. *J. Photochem. Photobiol. C* **2000**, *1*, 79.
(9) Bohn, R. K.; Sorenson, S. A.; True, N. S.; Brupbacher, T.; Gerry, M. C. K.; Jäger, W. *J. Mol. Spectrosc.* **1997**, *184*, 167.
(10) Tozer, D. J. *Chem. Phys. Lett.* **1999**, *308*, 160.
(11) Sadova, N. I.; Vilkov, L. V.; Hargittai, I.; Brunvoll, J. *J. Mol. Struct.* **1976**, *31*, 131.
(12) Scharfenberg, P. *J. Chem. Phys.* **1982**, *77*, 4791.
(13) Ribeiro-Claro, R. J. A.; Gonsalves, A. M. d'A. R.; Teixeira-Dias, J. J. C. *Spectrochim. Acta* **1985**, *41A*, 1055.
(14) Schaefer, T.; Sebastian, R.; Penner, G. H. *Can. J. Chem.* **1986**, *64*, 1372.
(15) Sorenson, S. A.; True, N. S. *J. Mol. Struct.* **1991**, *263*, 21.
(16) Benassi, R.; Bertarini, C.; Taddei, F. *J. Mol. Struct.* **1995**, *339*, 103.
(17) Im, H. S.; Bernstein, E. R.; Secor, H. V.; Seeman, J. I. *J. Am. Chem. Soc.* **1991**, *113*, 4422.
(18) Ichimura, T.; Mori, Y. *J. Chem. Phys.* **1972**, *57*, 1677.
(19) Lin, C. C.; Swalen, J. D. *Rev. Mod. Phys.* **1959**, *31*, 841.
(20) Lewis, J. D.; Malloy, T. B.; Chao, T. H.; Laane, J. *J. Mol. Struct.* **1972**, *12*, 427.
(21) Takemura, T.; Fujita, M.; Ohta, N. *Chem. Phys. Lett.* **1988**, *145*, 215.
(22) Frisch, M. J.; Trucks, G. W.; Schlegel, H. B.; Scuseria, G. E.; Robb, M. A.; Cheeseman, J. R.; Zakrzewski, V. G.; Montgomery, J. A., Jr.; Stratmann, R. E.; Burant, J. C.; Dapprich, S.; Millam, J. M.; Daniels, A. D.; Kudin, K. N.; Strain, M. C.; Farkas, O.; Tomasi, J.; Barone, V.; Cossi, M.; Cammi, R.; Mennucci, B.; Pomelli, C.; Adamo, C.; Clifford, S.; Ochterski, J.; Petersson, G. A.; Ayala, P. Y.; Cui, Q.; Morokuma, K.; Malick, D. K.; Rabuck, A. D.; Raghavachari, K.; Foresman, J. B.; Cioslowski, J.; Ortiz, J. V.; Stefanov, B. B.; Liu, G.; Liashenko, A.; Piskorz, P.; Komaromi, I.; Gomperts, R.; Martin, R. L.; Fox, D. J.; Keith, T.; Al-Laham, M. A.; Peng, C. Y.; Nanayakkara, A.; Gonzalez, C.; Challacombe, M.; Gill, P. M. W.; Johnson, B. G.; Chen, W.; Wong, M. W.; Andres, J. L.; Head-Gordon, M.; Replogle, E. S.; Pople, J. A. *Gaussian 98*, Revision A.9; Gaussian, Inc.: Pittsburgh, PA, 1998.
(23) Benassi, R.; Taddei, F. *J. Mol. Struct.* **1997**, *418*, 59.
(24) Kreiner, W. A.; Rudolph, H. D.; Tan, B. T. *J. Mol. Spectrosc.* **1973**, *48*, 86.
(25) Breen, P. J.; Warren, J. A.; Bernstein, E. R.; Seeman, J. I. *J. Chem. Phys.* **1987**, *87*, 1917.
(26) Murov, S. L.; Carmicaael, I.; Hug, G. L. *Handbook of Photochemistry*, 2nd ed., Revised and Expanded; Marcel Dekker: New York, 1993.